

Supplementary information:

Enhanced fire-retardancy of poly(ethylene vinyl acetate) electrical cable coatings containing microencapsulated ammonium polyphosphate as intumescent flame retardant

Yan Zhang^{a,b}, Bibo Wang^{a,}, Haibo Sheng^a, Bihe Yuan^a, Bin Yu^a, Gang Tang^c, Ganxin*

Jie^d, Hao Feng^d, Youji Tao^d, Yuan Hu^{a,b,}*

^aState Key Laboratory of Fire Science, University of Science and Technology of China, 96 Jinzhai Road, Hefei, Anhui 230026, People's Republic of China.

^bSuzhou Key Laboratory of Urban Public Safety, Suzhou Institute for Advanced Study, University of Science and Technology of China, 166 Ren'ai Road, Suzhou, Jiangsu 215123, People's Republic of China.

^cSchool of Architecture and Civil Engineering, Anhui University of Technology, 59 Hudong Road, Ma'anshan, Anhui 243002, People's Republic of China.

^dState Key Laboratory of Environmental Adaptability for Industrial Products, China National Electric Apparatus Research Institute Co., Ltd., Guangzhou 510663, People's Republic of China.

**Corresponding author. Fax/Tel: +86-551-63601664.*

E-mail address: yuanhu@ustc.edu.cn (Yuan Hu)

**Corresponding author. Fax/Tel: +86-551-63601664.*

E-mail address: wbibo@ustc.edu.cn (Bibo Wang)

Table S1. Formulations of MCAPP

Table S2. Element contents of APP and MCAPP.

Table S3. Mechanical properties of EVA-1 and EVA-2 in 0-6 weeks.

Table S4. LOI values of neat EVA in 0-6 weeks

Table S5. LOI values of APP, pentaerythritol, APP/pentaerythritol and MCAPP in EVA matrix.

Table S6. Related thermal degradation data of EVA-1 and EVA-2 under air atmosphere.

Fig. S1 Chemical structure of charring forming agent (CFA)

Fig. S2 (a) FTIR spectra of PETA, APTS, PETA-APTS and (b) ^1H NMR spectrum of PETA-APTS.

Fig. S3 Particle size distribution of APP, CFA and MCAPP

Fig. S4 XPS survey scans of APP and MCAPP.

Fig. S5 Digital images of EVA-1 and EVA-2 in 0-6 weeks.

Fig. S6 Representative tensile stress-strain curves of pristine EVA and its composites.

Fig. S7 Digital photographs for tensile samples of EVA-1 and EVA-2 in 0-6 weeks.

Fig. S8 Effect of hygrothermal ageing on the electrical properties of EVA-1 and EVA-2 in 0-6 weeks.

Fig. S9 (a) TGA and (b) DTG curves of EVA-1 and EVA-2 in 0 and 6 weeks under air condition.

Fig. S10 Absorbance of pyrolysis products for EVA-1 and EVA-2 in 0 and 6 weeks.

Fig. S11 SEM images of the surface for EVA-1 and EVA-2 tested for 0, 3, 6 weeks.

Table S1. Formulations of MCAPP

	APP	TEOS (SiO ₂ %=28.8%)	PETA-APTS
initial loading	1000.0 g	240.0 g	60.0 g
after encapsulation	1000.0 g	69.1 g	47.1 g
ratio	89.6%	6.2%	4.2%

PETA-APTS	PETA	APTS
initial loading	34.4 g	25.6 g
after encapsulation	34.4 g	12.7 g
ratio	3.1%	1.1%

Table S2. Element contents of APP and MCAPP.

Element	APP	MCAPP
C (at%)	16.31	18.33
P (at%)	11.21	6.21
N (at%)	28.41	8.41
O (at%)	44.07	57.46
Si (at%)	—	9.59
Total	100.00	100.00

Table S3. Mechanical properties of EVA-1 and EVA-2 in 0-6 weeks.

sample	Tensile strength (MPa)	Elongation at break (%)
EVA-1-0W	9.52 ± 0.25	447 ± 15
EVA-1-1W	7.43 ± 0.39	410 ± 8
EVA-1-2W	6.13 ± 0.40	312 ± 9
EVA-1-3W	7.80 ± 0.35	317 ± 7
EVA-1-4W	9.90 ± 0.23	368 ± 12
EVA-1-5W	9.80 ± 0.25	393 ± 4
EVA-1-6W	9.93 ± 0.15	390 ± 7
EVA-2-0W	13.67 ± 0.23	508 ± 5
EVA-2-1W	11.80 ± 0.34	429 ± 8
EVA-2-2W	11.70 ± 0.36	449 ± 7
EVA-2-3W	11.03 ± 0.25	459 ± 8
EVA-2-4W	10.47 ± 0.16	433 ± 15
EVA-2-5W	10.53 ± 0.18	413 ± 10
EVA-2-6W	10.90 ± 0.25	420 ± 6

EVA-2-
6W

Table S4. LOI values of neat EVA in 0-6 weeks

sample	EVA-0W	EVA-1W	EVA-2W	EVA-3W	EVA-4W	EVA-5W	EVA-6W
LOI	18	18	17.5	17.5	17	16.5	16.5

Table S5. LOI values of APP, pentaerythritol, APP/pentaerythritol and MCAPP in
EVA matrix.

	EVA1828	C328	APP	PER	TEOS-PETA-APTS	MCAPP	CFA	TAIC	1010	DSTP	LOI
EVA-PER	63.2%	4.8%		19.4%			9.7%	1.5%	0.7%	0.7%	19.0
EVA-1	63.2%	4.8%	19.4%				9.7%	1.5%	0.7%	0.7%	31.0
EVA-APP/PER	63.2%	4.8%	17.4%	2.0%			9.7%	1.5%	0.7%	0.7%	30.5
EVA-APP/TEOS-PETA-APTS	63.2%	4.8%	17.4%		2.0%		9.7%	1.5%	0.7%	0.7%	31.0
EVA-2	63.2%	4.8%				19.4%	9.7%	1.5%	0.7%	0.7%	33.0

Table S6. Related data of EVA-1 and EVA-2 under air atmosphere.

Sample	T _{-5wt%} (°C)	T _{max1} (°C)	T _{max2} (°C)	Residue at 600 °C (wt %)
EVA-1-0W	302.5	328.4	429.6	18.6
EVA-1-6W	291.5	326.1	429.1	16.3
EVA-2-0W	304.7	328.7	443.8	19.7
EVA-2-6W	287.0	327.6	434.2	19.3

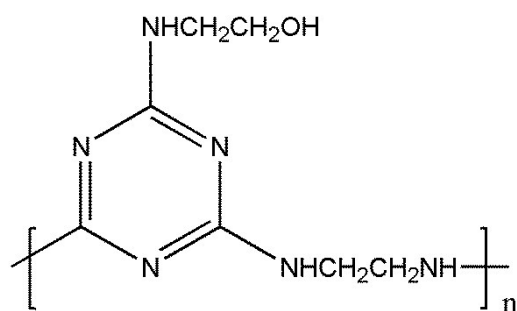


Fig. S1 Chemical structure of charring forming agent (CFA)

Synthesis of CFA¹:

Cyanuric chloride (1.0 mol) and water (400 mL) were fed into 1000 mL four-neck flask which was equipped with a stirrer, thermometer, dropping funnel, and reflux condenser. Ethanolamine (1.0 mol) and NaOH (1.0 mol) were mixed together in water

and then the mixed solution was added dropwise into the flask, and regulated the pH to 5–8 by the speed of the dropwise. The reaction was kept at 0–5 °C for 3 h.

After that, a water solution of ethylenediamine (0.5 mol) and NaOH (1.0 mol) was added to the above reactive system containing intermediate I and kept at pH = 5–8 by the speed of the dropwise of the alkali solution. The reaction was kept at 40–50 °C for 10 h.

Finally, another mixed water solution of both ethylene-diamine (0.5 mol) and NaOH (1.0 mol) was added to the above system containing intermediate II and was refluxed for 10 hr. It was then cooled to room temperature, and the product was filtered and washed with acetone and water. In this way the char forming agent was obtained.

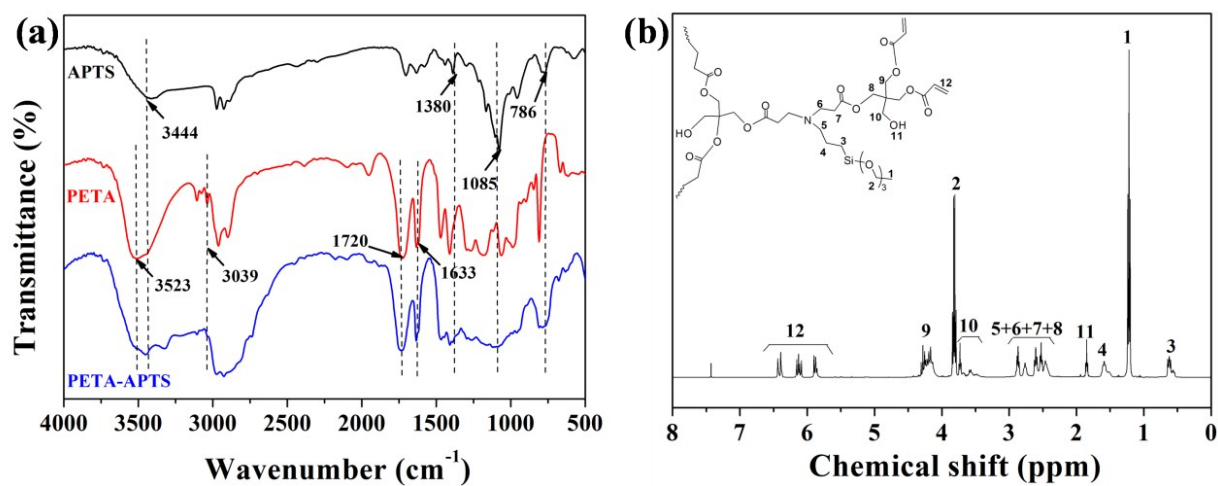


Fig. S2 (a) FTIR spectra of PETA, APTS, PETA-APTS and (b) ¹H NMR spectrum of PETA-APTS.

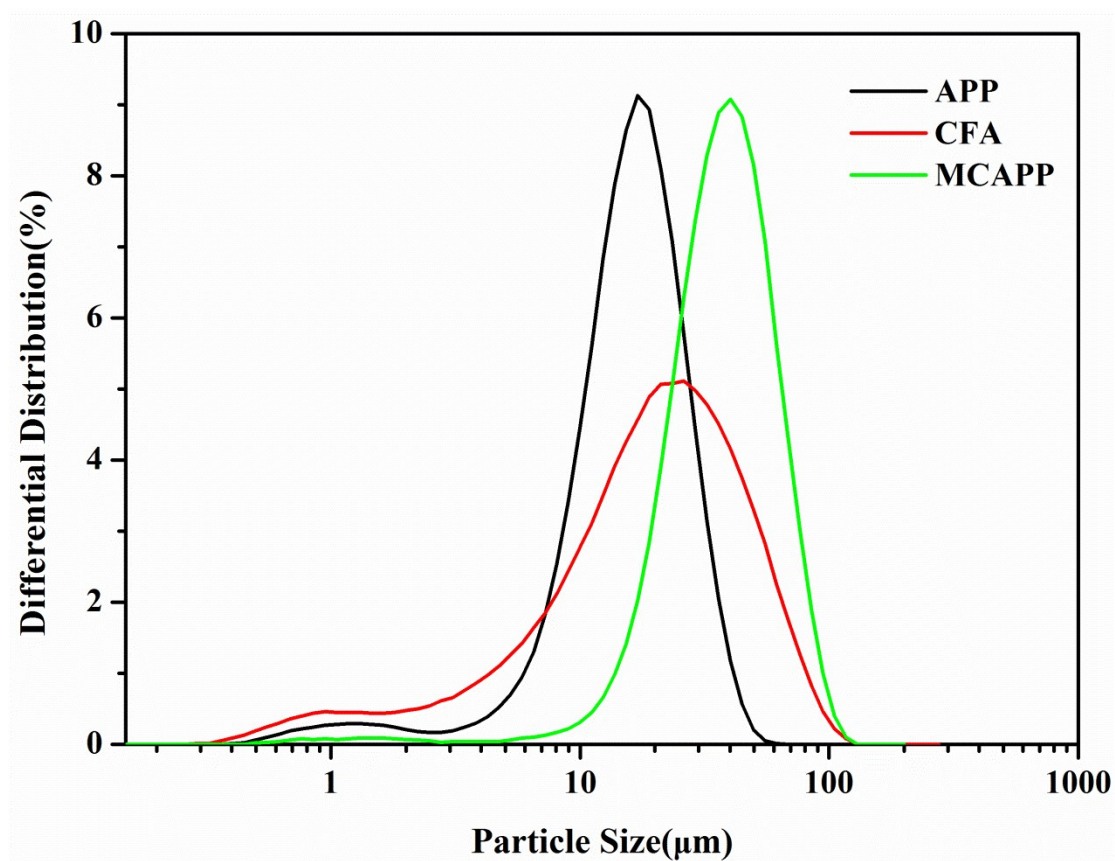


Fig. S3 Particle size distribution of APP, CFA and MCAPP

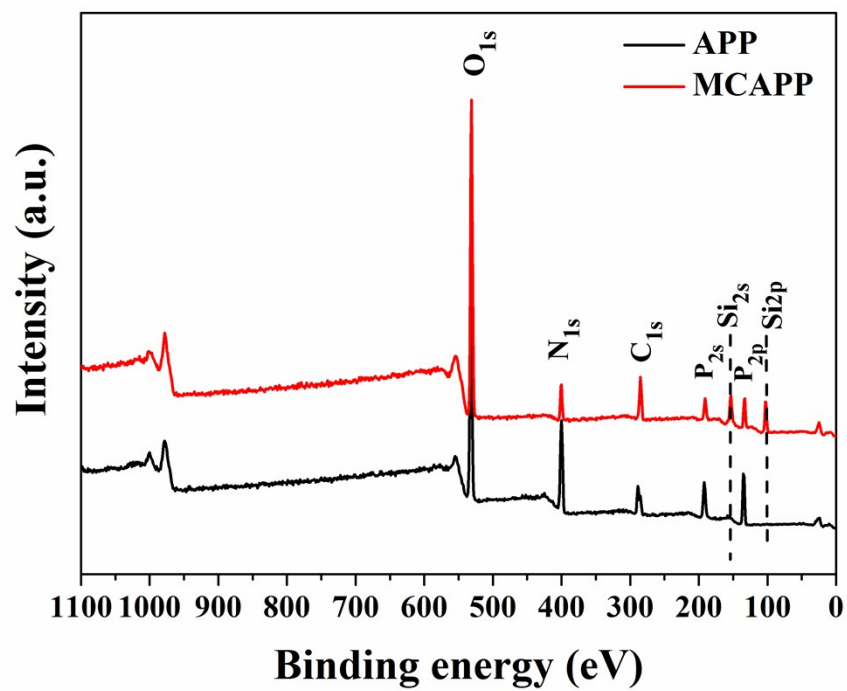


Fig. S4 XPS survey scans of APP and MCAPP.

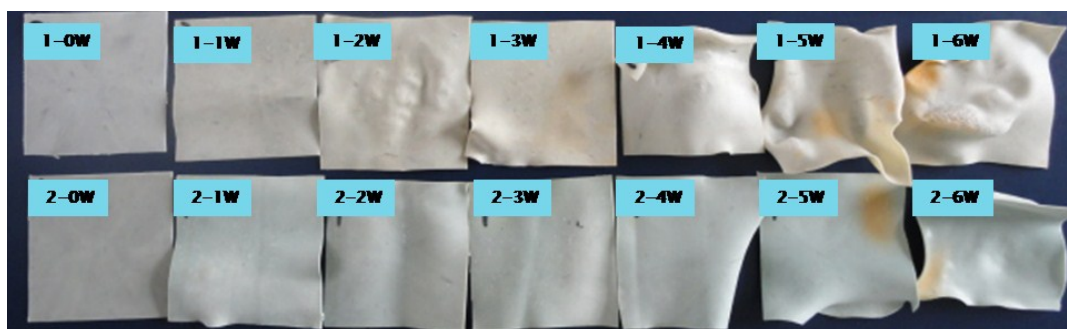


Fig. S5 Digital images of EVA-1 and EVA-2 in 0-6 weeks.

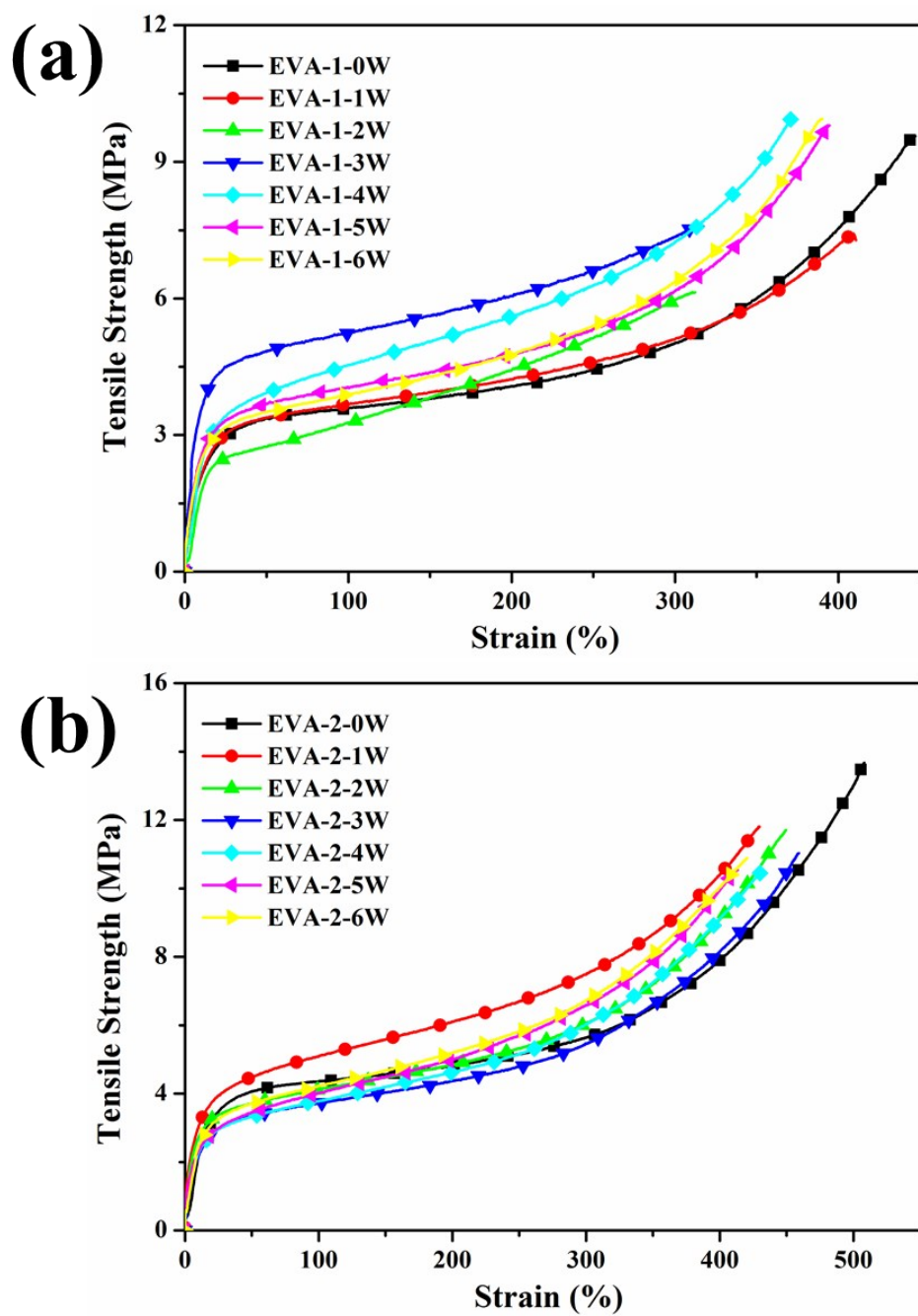


Fig. S6 Representative tensile stress–strain curves of pristine EVA and its composites.

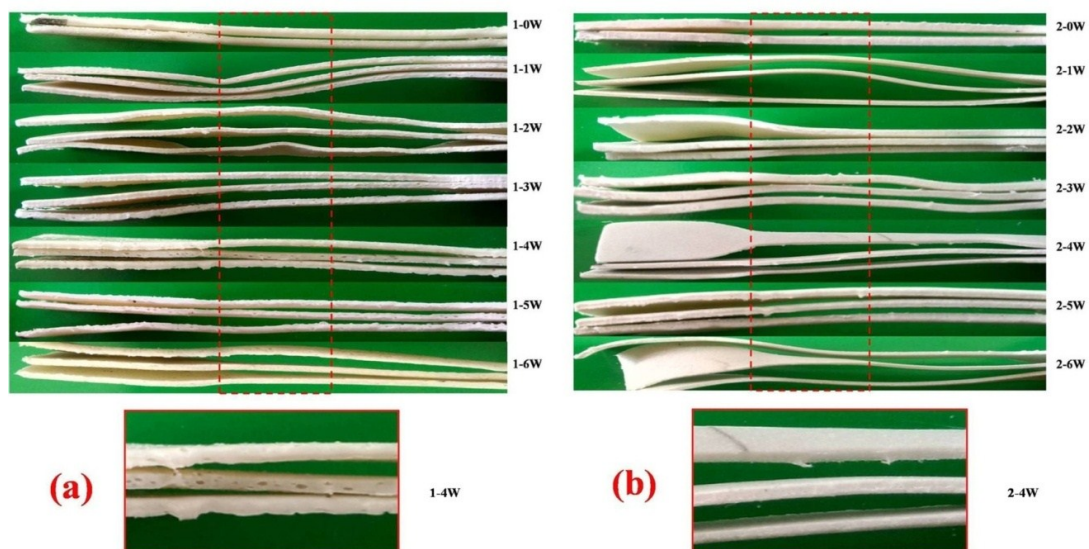


Fig. S7 Digital photographs for tensile samples of EVA-1 and EVA-2 in 0-6 weeks.

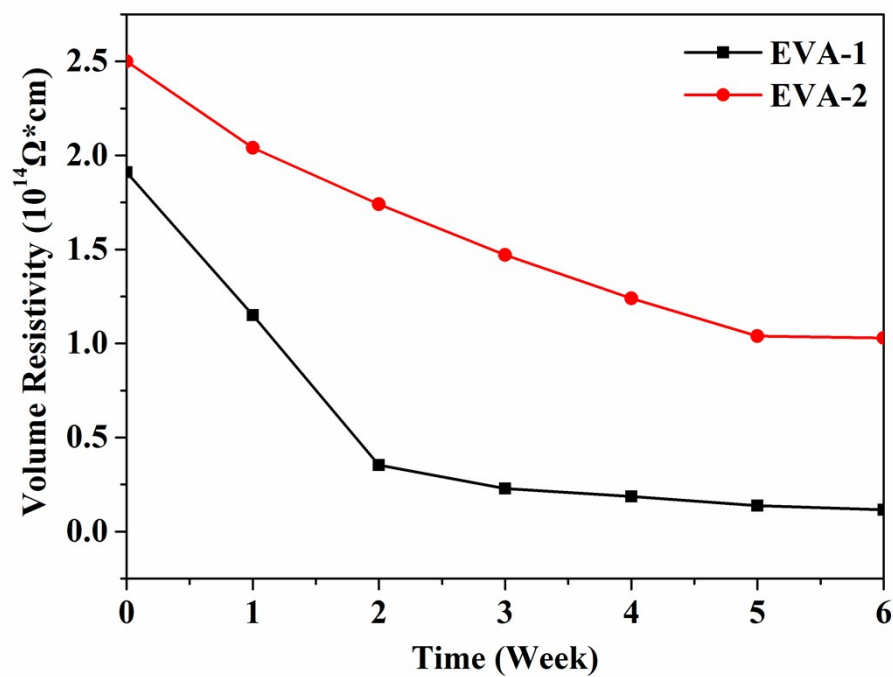


Fig. S8 Effect of hygrothermal ageing on the electrical properties of EVA-1 and EVA-2 in 0-6 weeks.

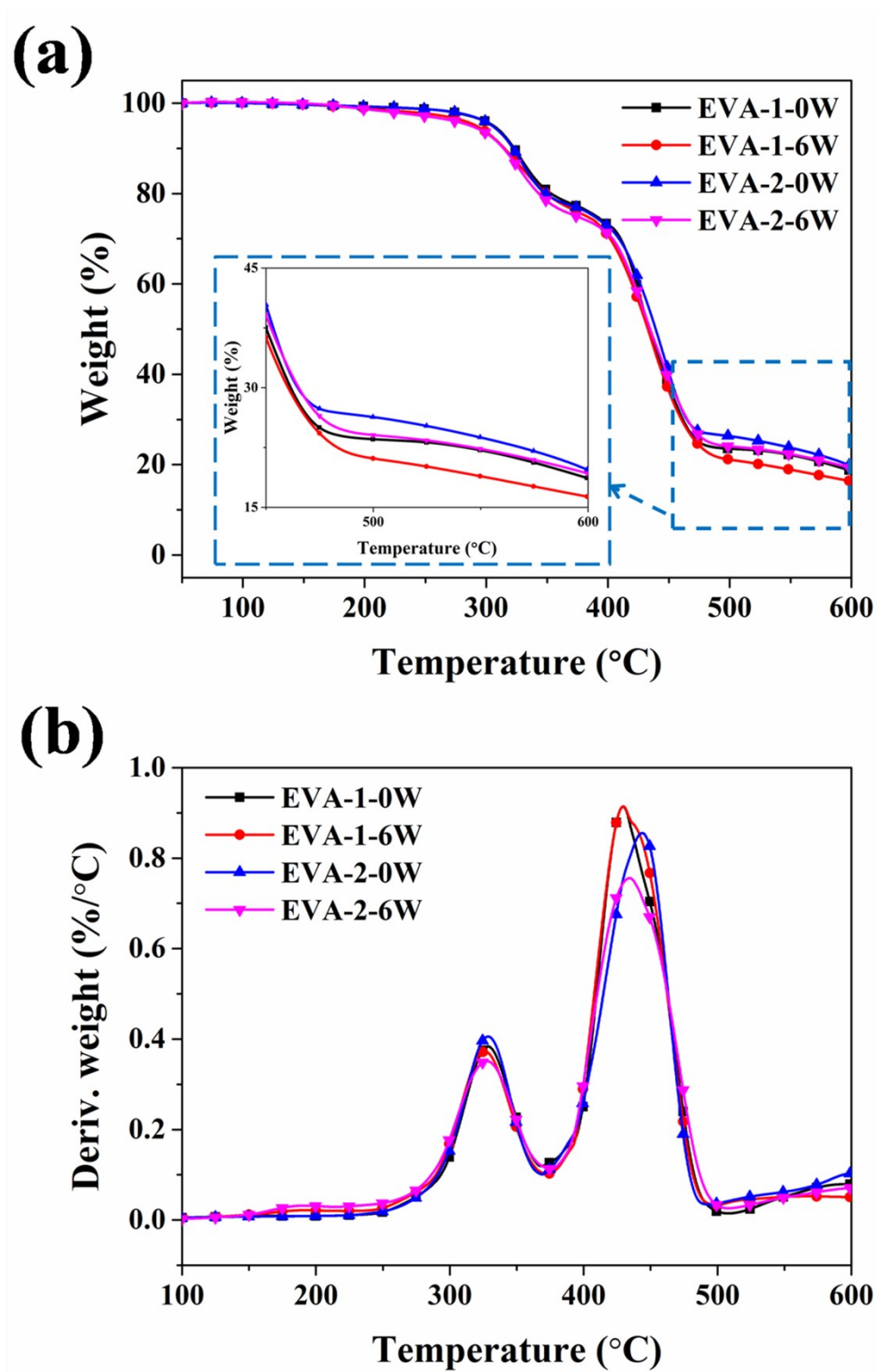


Fig. S9 (a) TGA and (b) DTG curves of EVA-1 and EVA-2 in 0 and 6 weeks under air condition.

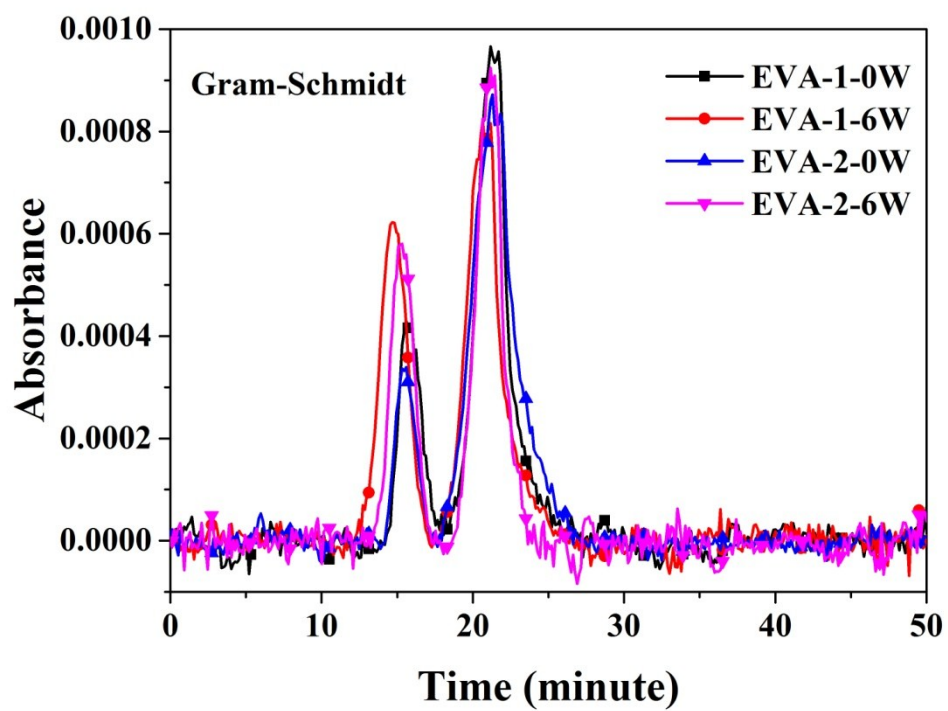


Fig. S10 Absorbance of pyrolysis products for EVA-1 and EVA-2 in 0 and 6 weeks.

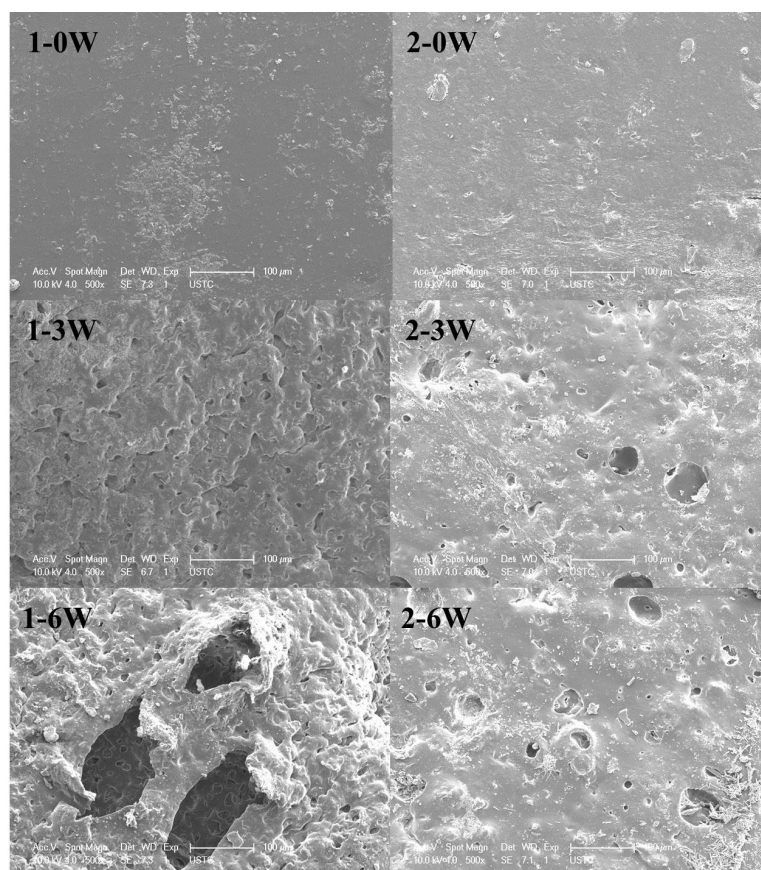


Fig. S11 SEM images of the surface for EVA-1 and EVA-2 tested for 0, 3, 6 weeks.

1. S. Nie, Y. Hu, L. Song, Q. He, D. Yang and H. Chen, *Polymers for Advanced Technologies*, 2008, **19**, 1077-1083.